Since January 2020 Elsevier has created a COVID-19 resource centre with free information in English and Mandarin on the novel coronavirus COVID-19. The COVID-19 resource centre is hosted on Elsevier Connect, the company's public news and information website.

European Journal of Pharmacology 883 (2020) 173374

Contents lists available at ScienceDirect

European Journal of Pharmacology

journal homepage: www.elsevier.com/locate/ejphar

Full length article

MicroRNA-122 aggravates angiotensin II-mediated apoptosis and autophagy imbalance in rat aortic adventitial fibroblasts via the modulation of SIRT6-elabela-ACE2 signaling

Juan-Juan Song [a], Mei Yang [a], Ying Liu [a], Jia-Wei Song [a], Juan Wang [a], Hong-Jie Chi [a], Xiao-Yan Liu [a,b], Kun Zuo [a], Xin-Chun Yang [a], Jiu-Chang Zhong [a,b,*]

[a] Heart Center and Beijing Key Laboratory of Hypertension, Beijing Chaoyang Hospital, Capital Medical University, Beijing, 100020, China
[b] Medical Research Center, Beijing Chaoyang Hospital, Capital Medical University, Beijing, 100020, China

ARTICLE INFO

Keywords:
MicroRNA-122-5p
Sirtuin 6
Elabela
Autophagy
Adventitial fibroblasts

ABSTRACT

Abnormal aortic adventitial fibroblasts (AFs) play essential roles in the development of vascular remodeling and disorders. Previous studies revealed that microRNA-122 (miR-122) levels were elevated in the aortic adventitia of hypertensive rats with vascular injury. Here, we aim to evaluate the biological effects and underlying mechanisms of miR-122 in rat AFs. Exposure to angiotensin II (ATII) in rat AFs resulted in decreased levels of sirtuin 6 (SIRT6), elabela (ELA), and angiotensin-converting enzyme 2 (ACE2). Additionally, stimulation with ATII contributed to a decline in autophagic flux and obvious increases in cellular migration, oxidative stress, and apoptosis, which were exacerbated by the transfection of miR-122-5p mimic but were rescued by miR-122-5p inhibitor, exogenous replenishment of ELA, and recombinant adeno-associated virus expressing SIRT6 (rAAV-SIRT6), respectively. Moreover, stimulation with miR-122-5p mimic led to a marked reduction in the levels of SIRT6 and ELA in rat AFs, which were elevated by stimulation with rAAV-SIRT6. Furthermore, miR-122-5p inhibitor-mediated pro-autophagic, anti-oxidant and anti-apoptotic effects in rat AFs were partially suppressed by 3-methyladenine, SIRT6 small interfering RNA (siRNA) and ELA siRNA, which were linked with the down-regulation in the protein levels of LC3-II, beclin-1, and ACE2 and the upregulation of p62 expression and bax/bcl-2 ratio. Our findings indicated that miR-122-5p inhibition prevented ATII-mediated loss of autophagy, and the promotion of apoptosis and oxidative stress via activating the SIRT6-ELA-ACE2 signaling. MiR-122-5p may be a novel predictive biomarker of adventitial injury, and targeting the SIRT6-ELA-ACE2 signaling may have the potential therapeutic importance of controlling vascular remodeling and disorders.

1. Introduction

Vascular remodeling is an elaborate pathophysiological process of the major adaptive mechanisms of hypertension, which is characterized as pathological hypertrophy of adventitial fibroblasts (AFs), the proliferation of medial smooth muscle cells (SMCs), dysregulation of intimal endothelial cells, inflammation of macrophage and the participation of extracellular matrix protein (Heeneman et al., 2007; Bersi et al., 2016; An et al., 2015). Intriguingly, adventitia is instrumental in regulating the structure and function of blood vessel walls, and excessive adventitial remodeling has been implicated in the process of hypertension, which is characterized as thickened adventitia, increased number of fibroblasts and phenotypic change of fibroblasts to myofibroblasts (Bersi et al., 2016). In response to vascular injury or stress, AFs are the first to be activated and reprogrammed to exert regulatory effects on the structure and function of vascular walls (An et al., 2015). Both sirtuin 6 (SIRT6) and elabela (ELA)/apelin receptor (APJ) signaling appear to be crucial to normal vasculature development and have emerged as key regulators of vascular cell proliferation, apoptosis, and inflammation (Yang et al., 2017, 2019; Zhang et al., 2017a). SIRT6 prevents vascular endothelial cells against angiotensin II (ATII)-mediated apoptosis and oxidative stress by the activation of nuclear factor erythroid 2-related factor 2/anti-oxidant response elements redox signaling (Yang et al., 2019). ELA is a novel endogenous ligand of APJ and exhibits a similar vascular

* Corresponding author. Heart Center and Beijing Key Laboratory of Hypertension, Beijing Chaoyang Hospital Affiliated to Capital Medical University, Beijing, 100020, China.
E-mail addresses: jczhong@sina.com, jiuchangzhong@aliyun.com (J.-C. Zhong).

https://doi.org/10.1016/j.ejphar.2020.173374
Received 20 March 2020; Received in revised form 11 July 2020; Accepted 13 July 2020
Available online 16 July 2020

profile with apelin in the pathogenesis of hypertension and other vascular diseases. Exogenous ELA has been shown to improve vascular remodeling in pulmonary artery hypertension (Yang et al., 2017). However, the exact roles of SIRT6 signaling and the ELA-APJ axis in vascular injury and disorders remain poorly unknown.

MicroRNAs (miRNAs) are small, conserved, single-stranded, non-coding RNA molecules that bind to complementary sites located on the 3′-untranslated region (3′-UTR) of their target mRNAs, which thereby trigger either translational repression or RNA degradation (Kataoka and Wang, 2014). MiRNAs are highly expressed in AFs, and play critical roles in the regulation of vascular cell growth, differentiation, apoptosis, and autophagy (Hynes et al., 2012; De Rosa and Indolfi, 2015; Xu et al., 2016). Notably, microRNA-122 (miR-122) has been proposed as a biomarker of cardiovascular diseases such as atherosclerosis, acute coronary syndrome, and heart failure, which are all involved in arterial remodeling (De Rosa and Indolfi, 2015; Xu et al., 2016). Our previous study suggested that pressure overload by transverse aorta constriction (TAC) resulted in the pathological adventitial remodeling of rat ascending aortas, which was linked with increased levels of miR-122 and reduced levels of the apelin-APJ system (Xu et al., 2016). However, the regulatory roles of miR-122 in adventitial cells remain to be clarified. In this study, we aim to investigate the regulatory roles and underlying mechanisms of miR-122 in SIRT6 and ELA-APJ signaling in rat AFs in response to ATII.

2. Materials and methods

2.1. Isolation and culture of primary rat AFs

The protocol of the study was approved by the Animal Research Ethics Committee of Beijing Chaoyang Hospital affiliated to Capital Medical University (approval number:2017-K-132) in China. Primary rat AFs were isolated from ascending aortas of 5- to 6-week-old male Sprague-Dawley rats (Charles River, China, License number: SCXK (Beijing) 2016-0006) as described previously (Xu et al., 2016). Briefly, the rats were anesthetized with chloral hydrate and immediately decapitated. Under aseptic conditions, the adventitia was carefully removed from the thoracic aortas of rats, and the medial and intimal layers were separated from the adventitia. The remaining adventitia was cut into tissue sections (1 mm^3) and plated in Dulbecco's modified Eagle's medium supplemented with 20% heat-inactivated fetal bovine serum, 1% L-glutamine, 100 U/ml penicillin, and 100 mg/ml streptomycin. The explants were incubated in a humidified atmosphere of 5% CO_2 and 95% air at 37 °C until the cells reached a confluence level of 80% for passage. The cell morphology of AFs derived from the adventitia of the aorta was observed under a microscope. The AFs were then stained with vimentin (a marker of fibroblasts), and α-smooth muscle actin (α-SMA; a marker of SMCs) using immunofluorescence analysis. The rat AFs from the third to sixth generation were used in subsequent experiments. The subconfluent cells were made quiescent through incubation of the AFs in a serum-free medium for 24 h before stimulation. Then, recombinant human ELA-32 (100 nM), adenosine 5′-monophosphate-activated protein kinase (AMPK) agonist 5-amino-4-imidazole carboxamide riboside (AICAR; 100 μM), mammalian target of rapamycin (mTOR) inhibitor rapamycin (1 mM), and autophagy inhibitor 3-methyladenine (10 mM) were added to AFs for 1 h followed by 24 h exposure to ATII (100 nM), respectively.

2.2. Cell transfection, wound-healing assay, and dihydroethidium staining

MiR-122-5p mimic, miR-122-5p inhibitor, specific small interfering RNAs (siRNAs) targeting ELA-32, SIRT6, and angiotensin-converting enzyme 2 (ACE2) and corresponding negative control (NC) siRNAs (GenePharma, Shanghai, China) were transiently transfected into AFs for 48 h at a concentration of 50 nM using Lipofectamine 3000 reagent (Invitrogen, CA, USA). The recombinant adeno-associated viruses expressing SIRT6 (rAAV-SIRT6) and green fluorescent protein (rAAV-GFP) were provided by Genechem (Shanghai, China). The AFs were transduced with rAAV-SIRT6 (1×10^{12} pfu/ml) and rAAV-GFP (1×10^{12} pfu/ml) and continued to be passaged and cultured for 5–7 days. The intensity of green fluorescence was determined to verify the successful transfection into AFs under a fluorescence microscope. ATII (100 nM) was then added to rat AFs for 24 h. For wound healing assay, wounds were made by scratching with a pipette tip, and photographs were taken immediately (0 h) and 24 h after wounding as previously described (Zhang et al., 2017b). After wounding for 24 h, rat AFs were washed with a phosphate-buffered solution (PBS) and photographed to examine the migration of AFs into the middle line of the scratch. The scratch area was calculated using Image J software and the relative migration index was obtained from the ratio of cell migration distance at 0 h and 24 h with (migration distance at 0 h-migration distance at 24 h)/migration distance at 0 h. Dihydroethidium fluorescence staining was performed to monitor the production of reactive oxygen species. The AFs pre-treated with ATII (100 nM) were incubated with 10 mM reactive oxygen species inhibitor N-acetyl-L-cysteine (NAC) at 37 °C for 30 min and followed by exposure to dihydroethidium (20 μM) for 30 min. The cell plates were wrapped with foil to minimize exposure to light. Additionally, one cell plate was kept without dihydroethidium as a blank control. Fluorescent images were captured with an Olympus IX51 microscope (Olympus, Tokyo).

2.3. Immunofluorescence analysis and flow cytometry

AFs were seeded in Φ35 mm confocal Petri dishes with a glass-bottom diameter of 20 mm at a density of 5×10^4 cells/well, fixed in 4% paraformaldehyde (paraformaldehyde, phosphate and deionized water with a pH of 7.4) for 15 min, permeabilized in 0.1% Triton X-100 for 20 min, and then blocked with 0.5% goat serum in PBS. AFs were incubated with primary antibodies against light chain 3 (LC3), and p62 (Abcam, CA, USA) at 4 °C overnight and then incubated with secondary antibodies for 1 h. Finally, the nuclei were stained with flourished mounting medium with DAPI (Invitrogen, USA) intended for mounting slides and forming a semi-permanent seal for prolonged storage of slides at 4 °C for 10 min. Fluorescent images were captured by an Olympus IX51 microscope (Olympus, Tokyo). To investigate cell survival, AFs were washed with PBS and stained with Annexin V-FITC and propidium iodide (PI) detection kit (BD, USA). Briefly, the cells were resuspended in 100 μl binding buffer solution containing 5 μl Annexin V-FITC and 5 μl PI in the dark for 15 min and then analyzed by flow cytometry within 1 h after halting reaction. NRCMs and H9C2 cells stained with Annexin V, PI, or both were designated early apoptotic, necrotic, or late apoptotic cells. The flow cytometry data were analyzed using FlowJo V10 software.

2.4. Western blot analysis

Western blot analysis was conducted in rat AFs as described previously (Xu et al., 2016; Zhang et al., 2017b). Equal amounts of proteins were collected, separated by sodium dodecyl sulfate-polyacrylamide gel electrophoresis, and transferred to polyvinylidene fluoride membrane (Millipore, USA). The membrane was blocked with 5% non-fat milk for 1 h and incubated overnight at 4 °C with primary antibodies against p-mTOR (#2971), mTOR (#2972), Bax (#2772), Bcl-2 (Sc-7382), Caspase-3 (#9662), p-AMPKα (#4184), AMPKα (#2532), SIRT6 (#12486), ACE2 (ab108252), P62 (ab56416), Beclin-1 (#3495), LC3B (ab192890), and GAPDH (#2118), respectively. The membrane was then incubated with HRP-labeled secondary antibodies (Invitrogen, USA) at room temperature for 1 h. In our study, we provided a reference for the use of GAPDH protein as a normalizing standard for western blotting. Antibodies were obtained from Cell Signaling Technology (Beverly, MA), Santa Cruz Biotechnology (Santa Cruz, CA) and Abcam Inc (Cambridge, MA), respectively. The intensity of blots was analyzed

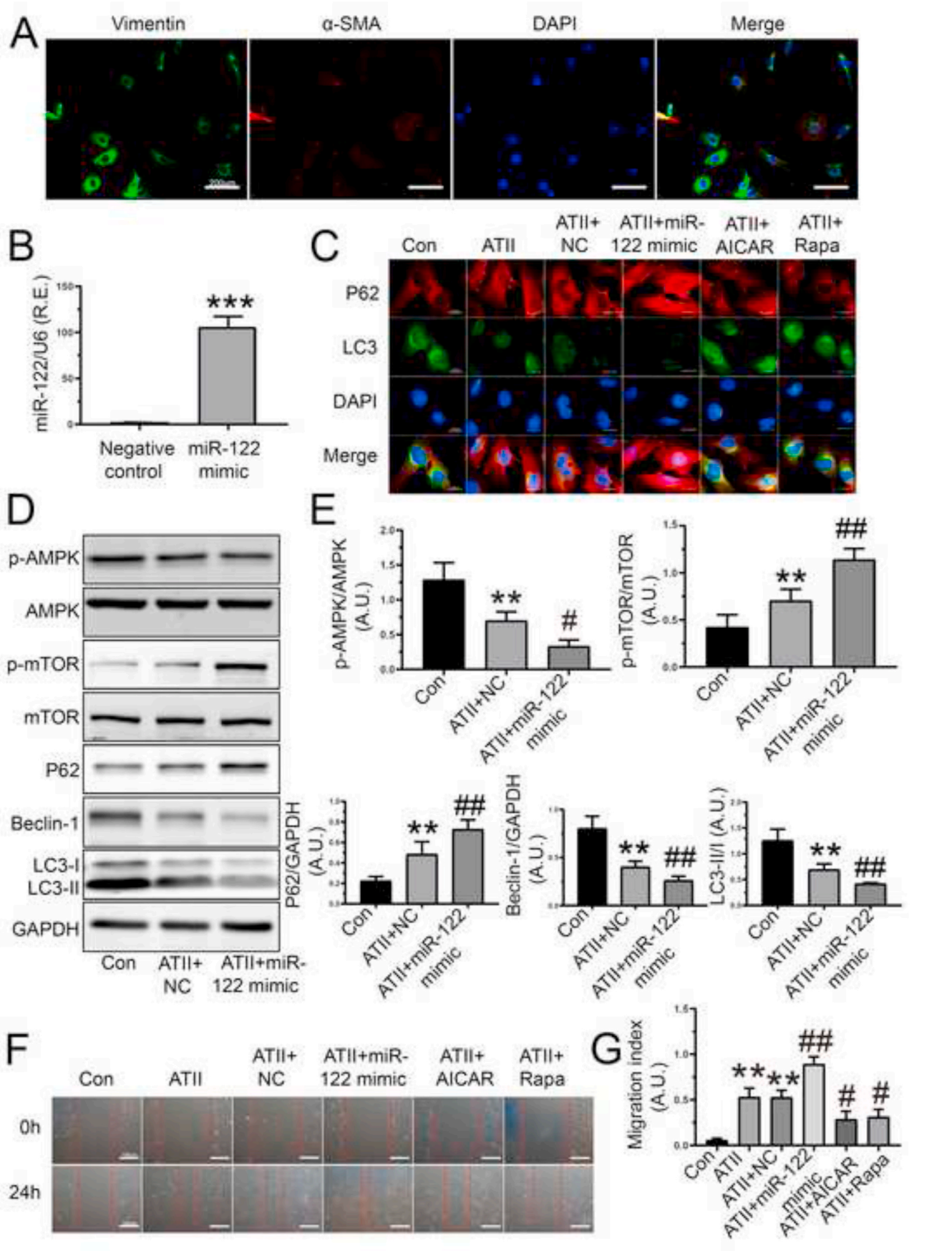

(caption on next page)

Fig. 1. Regulatory roles of miR-122-5p mimic in cellular autophagy and migration in rat AFs. (A) Representative images of immunofluorescence staining of vimentin (green) and α-SMA (red) in rat AFs. (B) The relative mRNA level of miR-122-5p in rat AFs after the transfection of miR-122-5p mimic. U6 was used as an endogenous control. (C) Immunofluorescence staining array of LC3 (green) and p62 (red) in rat AFs pre-treated with ATII, NC, miR-122-5p mimic, AICAR, and Rapa, respectively. (D-E) Representative western blots images and quantification in rat AFs after stimulation with miR-122-5p mimic. GAPDH was used as an endogenous control. (F-G) *In vitro* wound healing images with quantification in rat AFs in 0 h and 24 h, respectively. n = 3–4 for each group except for B where n = 6. **, $P < 0.01$, ***, $P < 0.001$ compared with control or NC group; #, $P < 0.05$, ##, $P < 0.01$ compared with ATII or ATII + NC group. A.U., arbitrary units; R.E., relative expression; NC, negative control; AFs, adventitial fibroblasts; ATII, angiotensin II; AICAR, 5-amino-4-imidazole carboxamide riboside; Rapa, rapamycin; α-SMA, α-smooth muscle actin; DAPI, 4′,6′-diamidino-2-phenylindole.

using Image J software.

2.5. Quantitative reverse transcription-polymerase chain reaction (qRT-PCR)

The qRT-PCR array was performed in AFs as described previously (Xu et al., 2016; Zhang et al., 2017b). Total RNAs containing miRNAs were isolated from rat AFs using TRIzol reagent (Invitrogen, USA) and reversely transcribed into cDNAs with PrimeScript reverse transcription reagent kit (Takara, Japan). Then, cDNAs were used for real-time fluorescent quantitative RT-PCR analysis to examine the expression of miR-122-5p, SIRT6, ELA, ACE2, interleukin 10 (IL-10), IL-18, and IL-33. The mRNA levels were measured using the ABI Prism 7500 sequence detection system (Applied, Biosystems, CA). The sequences of the primers used were as follows: rat miR-122-5p: forward 5′-CGATACAGAGAAGATTAGCATGGC-3′ reverse 5′-CCTGGAGTGT-G-ACAATGGTGTTTG-3’; SIRT6: forward 5′-CAGTGTTGGTGAT GTCGGTG-3′ reverse 5′-TGGGTCGAATATCTCGGGCA-3’; ELA: forward 5′-GTCACTGATCTCCTTGGTTA-3′ reverse 5′-TGCTCTAGTC-TAGTCTGTCT-3’; ACE2: forward 5′-CTTACGAGCCTCCTGTCACC-3′ reverse 5′-ATGCCAACCACTACCGTTCC-3’; IL-10: forward 5′-TTGAACCACCCGGCATCTAC-3′ reverse 5′-CCAAGGAGTTGCT CCCGTTA-3’; IL-18: forward 5′-CAGCCAACGAATCCCAGACC-3′ reverse 5′-ACAGATAGGGTCACAGCCAG-3’; IL-33: forward 5′-AGGTGCT ACTCCGTTACTACGA-3′ reverse 5′-GCGGAGAGAC- ATCACCCTTT-3’; GAPDH: forward 5′-AGTGCCAGCCTCGTCTCATA-3′ reverse

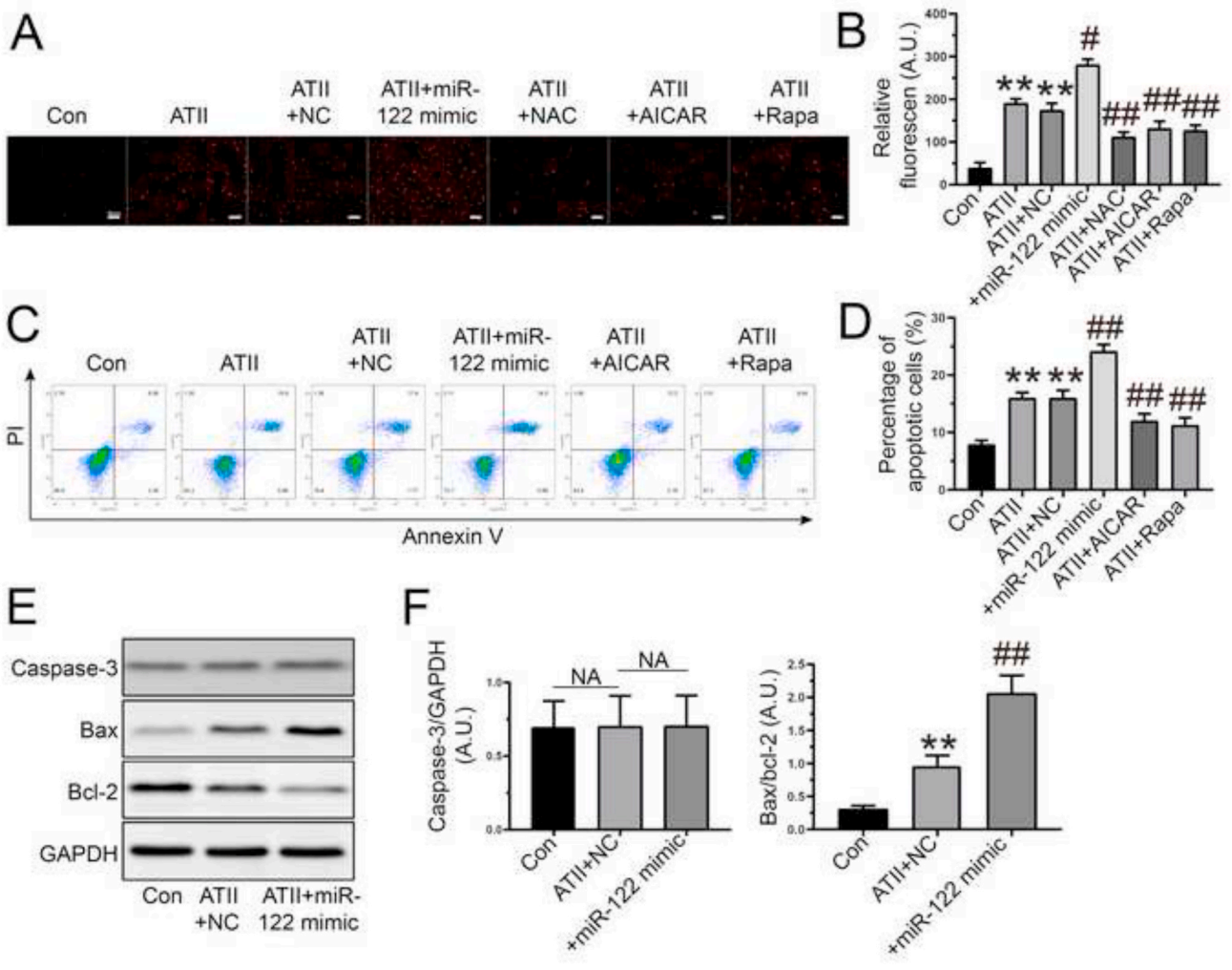

Fig. 2. Regulatory roles of miR-122-5p mimic in oxidative stress and apoptosis in rat AFs. (A-B) Representative dihydroethidium staining images with quantification in rat AFs in the absence and presence of ATII, NC, miR-122-5p mimic, NAC, AICAR, and Rapa, respectively. (C-D) Percentage of apoptotic cells by flow cytometry. (E-F) Representative western blots with quantification to examine the protein levels of caspase-3, bax, and bcl-2. GAPDH was used as an endogenous control. n = 3–4 for each group. **, $P < 0.01$ compared with control group; #, $P < 0.05$, ##, $P < 0.01$ compared with ATII or ATII + NC group. A.U., arbitrary units; AFs, adventitial fibroblasts; NC, negative control; ATII, angiotensin II; NAC, N-acetyl-L-cysteine; AICAR, 5-amino-4-imidazole carboxamide riboside; Rapa, rapamycin; NA, no statistical significance.

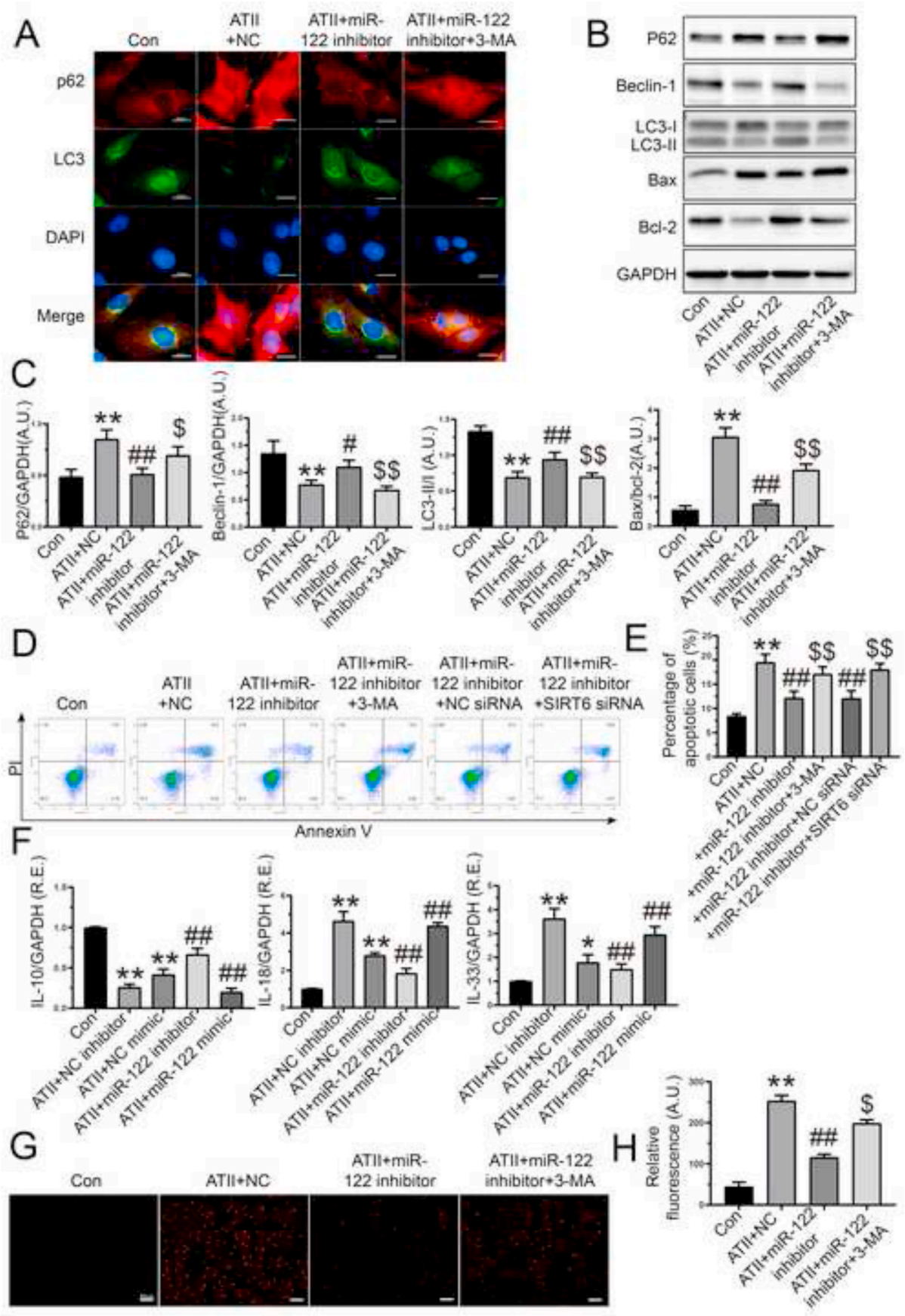

(caption on next page)

Fig. 3. Effects of miR-122-5p inhibitor on autophagy, apoptosis, inflammation, and oxidative stress in rat AFs. (A) Representative immunofluorescence images of p62 (red) and LC3 (green) in rat AFs in response to ATII, NC, miR-122-5p inhibitor, 3-MA, respectively. (B-C) Representative Western blots with quantification to detect protein levels of biomarkers of autophagy and apoptosis of rat AFs, respectively. (D-E) Flow cytometry to examine cellular apoptosis of AFs. (F) Relative mRNA levels of IL-10, IL-18, and IL-33 in rat AFs with qRT-PCR analysis. (G-H) Representative dihydroethidium staining with quantification to detect reactive oxygen species of rat AFs. GAPDH was used as an endogenous control. n = 3–4 for each group except for F where n = 5–6. *, $P < 0.05$, **, $P < 0.01$ compared with control group; #, $P < 0.05$, ##, $P < 0.01$ compared with ATII + NC group; $, $P < 0.05$, $$, $P < 0.01$ compared with ATII + miR-122 inhibitor or ATII + miR-122 inhibitor + NC siRNA group. A.U., arbitrary units; R.E., relative expression; NC, negative control; ATII, angiotensin II; AFs, adventitial fibroblasts; 3-MA, 3-methyladenine; IL-10, interleukin-10; IL-18, interleukin-18; IL-33, interleukin-33. SIRT6, sirtuin 6.

5′-TGAACT-TGCCGTGGGTAGAG-3’; U6: forward 5′-CGATACAGAG AAGATTAGCATGGC-3′ reverse 5′-AACGCTT CACGAATTTGCGT-3’. We provided a reference for the use of GAPDH transcript as a normalizing standard for all the target genes in rat AFs except for miR-122-5p that was normalized with a U6 snRNA transcript. The cycle number at which the reaction crossed an arbitrarily placed threshold (CT) was determined and relative mRNA levels were quantified using the $2^{-\triangle\triangle CT}$ method.

2.6. Statistical analysis

All results were presented as mean ± standard deviation (S.D). Significant differences were determined by Student’s t-test (for unpaired samples) or one-way analysis of variance (ANOVA) followed by a post hoc Bonferroni test using SPSS Statistics Version 24.0 software. Differences with a value of $P < 0.05$ were considered statistically significant.

3. Results

3.1. MiR-122-5p mimic accelerated ATII-mediated loss of autophagy and promotion of migration in rat AFs

To investigate the regulatory roles of miR-122-5p mimic, we firstly evaluated the effects of miR-122-5p mimic on autophagy and cellular migration in rat AFs. Representative images of immunofluorescence staining of vimentin and α-SMA were performed to ensure the purity of fibroblasts in cultured rat AFs (Fig. 1A). Notably, the relative mRNA level of miR-122-5p was markedly elevated in rat AFs after the transfection of miR-122-5p mimic (Fig. 1B). LC3-I-to-LC3-II conversion is the most widely used as autophagosome marker since the amount of LC3-II/LC3-I reflects the number of autophagosomes and the degradation of p62 is another biomarker to monitor autophagic activity. Beclin-1 functions as an autophagy initiation factor through interaction with phosphatidylinositol 3-kinase (PI3K). Additionally, AMPK is a negative regulator of mTOR and severs as a pro-autophagic factor in different cell types (Huang and Klionsky, 2007). In response to ATII, a loss of autophagic flux was determined in rat AFs, which was rescued by AMPK agonist AICAR and mTOR inhibitor rapamycin (Fig. 1C). Intriguingly, ATII-mediated loss of autophagy in rat AFs was further reduced by miR-122-5p mimic (Fig. 1C), which was associated with lower protein levels of beclin-1, LC3-II, and p-AMPK as well as higher expression of p62 and p-mTOR (Fig. 1D and E). Furthermore, the capability of cellular migration was increased in rat AFs after stimulation with ATII, which was decreased by AICAR and rapamycin, respectively (Fig. 1F and G). Conversely, ATII-induced pro-migratory action was enhanced in rat AFs after the transfection of miR-122-5p mimic (Fig. 1F and G). Therefore, these findings demonstrated that miR-122-5p mimic accelerated ATII-mediated loss of autophagy and promotion of cellular migration in rat AFs by modulating the AMPK/mTOR phosphorylation signaling.

3.2. MiR-122-5p mimic exacerbated ATII-mediated oxidative stress and apoptosis in rat AFs

The production of reactive oxygen species in cells induces membrane structural damage and the expression of apoptosis factors, including anti-apoptotic factors (bcl-2, bcl-x, bcl-w) and pro-apoptotic factors (bax, bak, bok), to regulate the caspase family and DNA degradation that can affect cell survival (Intengan and Schiffrin, 2001). Thus, we investigated the impacts of miR-122-5p on oxidative stress and apoptosis in rat AFs. Dihydroethidium staining and flow cytometry analysis revealed that cellular oxidant injury (Fig. 2A and B) and apoptosis (Fig. 2C and D) were significantly increased in rat AFs in response to ATII, which were reduced by treatment with NAC, AICAR, and rapamycin, respectively. Importantly, administration of miR-122-5p mimic enhanced ATII-mediated oxidative stress (Fig. 2A and B) and apoptosis (Fig. 2C and D) in rat AFs. Moreover, the bax/bcl-2 ratio was improved in rat AFs after exposure to ATII, which were further elevated after the transfection of miR-122-5p mimic (Fig. 2E and F). However, there was no difference in the expression of caspase-3 among groups (Fig. 2E and F). Taken together, these data suggested that miR-122-5p exacerbated ATII-mediated pro-oxidant and pro-apoptotic actions in rat AFs.

3.3. Inhibition of miR-122-5p prevented ATII-induced loss of autophagy and enhancements of apoptosis, inflammation and oxidative stress in rat AFs

To further verify the roles of miR-122-5p in rat AFs, we determined the effects of miR-122-5p inhibitor on ATII-mediated actions. Treatment with miR-122-5p inhibitor effectively prevented ATII-induced loss of autophagy (Fig. 3A), which were linked with the upregulation in the protein levels of beclin-1 and LC3-II and the downregulation of p62 expression (Fig. 3B and C). Conversely, the miR-122-5p inhibitor-mediated pro-autophagic effect was partially suppressed by 3-methyladenine (Fig. 3A, B, and C). Both Western blotting (Fig. 3B and C) and flow cytometry analysis (Fig. 3D and E) revealed that ATII-induced cellular apoptosis was prevented in rat AFs after the transfection of miR-122-5p inhibitor, which was enhanced by 3-methyladenine. Inflammation has been implicated in the initiation and progression of vascular diseases (Ridker et al., 2000). In this study, stimulation with ATII upregulated the expression of IL-18 and IL-33 but downregulated the mRNA level of IL-10 in rat AFs. Moreover, the ATII-induced pro-inflammatory action in AFs was enhanced by miR-122-5p mimic (Fig. 3F). In contrast, miR-122-5p inhibitor contributed to a marked decrease in the expression of IL-18 and IL-33 but an increase in the level of IL-10 in rat AFs (Fig. 3F). Additionally, the pro-oxidant effect of ATII in rat AFs was partially suppressed by miR-122-5p inhibitor, which was elevated by co-treatment with 3-methyladenine (Fig. 3G and H). Collectively, these data indicated that inhibition of miR-122-5p prevented ATII-induced anti-autophagic, pro-apoptotic, pro-inflammatory, and pro-oxidant roles in rat AFs.

3.4. Protective roles of miR-122-5p inhibition in controlling oxidative stress, cellular migration and autophagy in rat AFs via the activation of SIRT6 signaling

SIRT6 has been reported to be a target for miR-122-5p regulation by dual-luciferase reporter assay (Elhanati et al., 2016). To explore the regulatory mechanism of miR-122-5p on SIRT6, the bioinformatics software of miRNAs (TargetScanHuman 7.2 and microrna.org) were used to predict the target binding sites between miR-122-5p and 3′-UTR of SIRT6 mRNA (Fig. 4A). To verify the bioinformatics-based prediction, we measured the expression of SIRT6 in rat AFs with qRT-PCR and Western blot analysis after transfection of miR-122 mimic and inhibitor, respectively. Stimulation with ATII downregulated the mRNA and

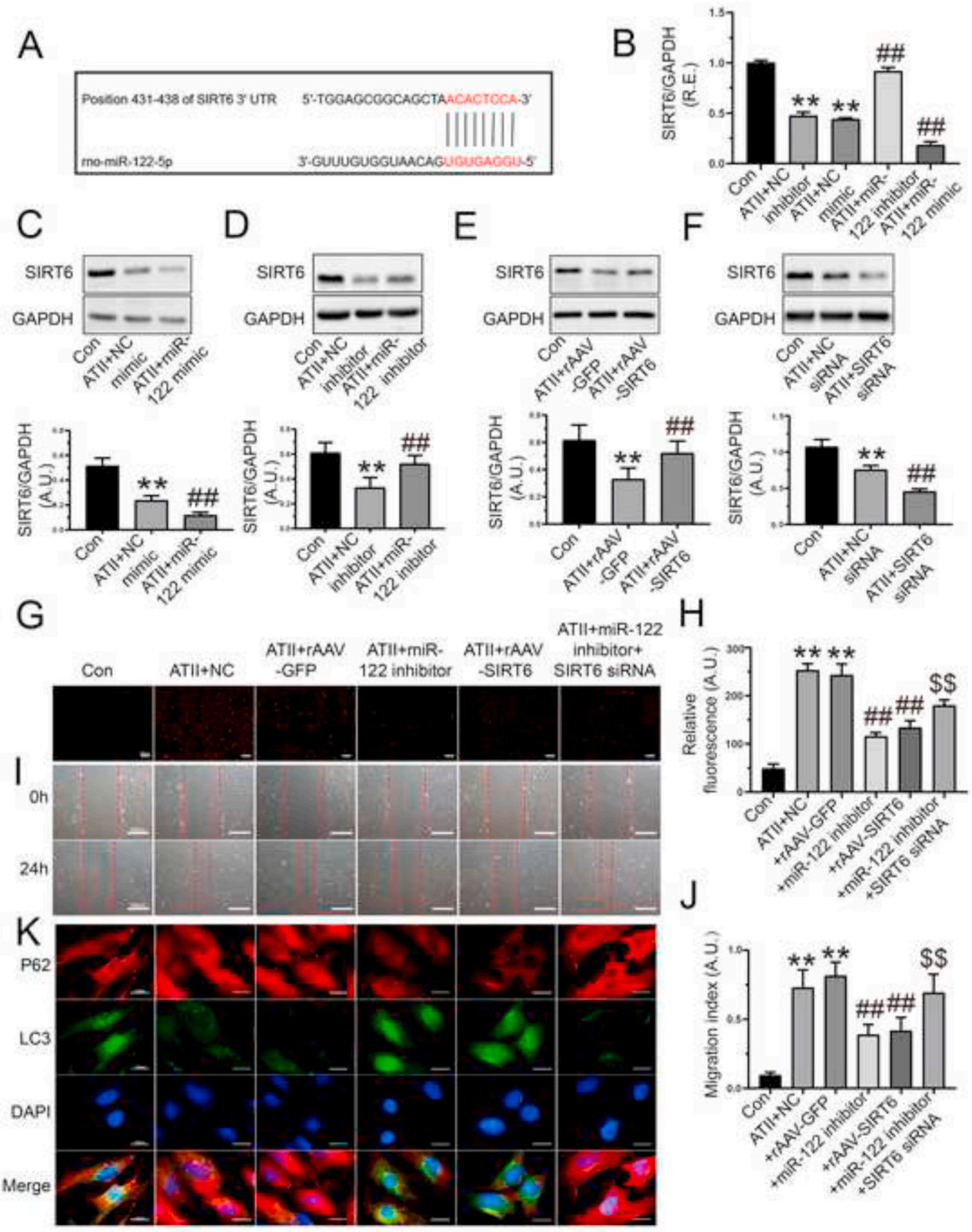

Fig. 4. Treatment with miR-122-5p inhibitor prevented ATII-mediated promotion of oxidative stress, migration, and loss of autophagy in rat AFs. (A) The binding sites between miR-122-5p and 3′-UTR of SIRT6 mRNA. (B) Relative mRNA level of SIRT6 in rat AFs by qRT-PCR analysis. (C-D) Western blots to examine protein levels of SIRT6 in AFs after the transfection of miR-122-5p mimic and inhibitor, respectively. (E-F) Protein levels of SIRT6 in rat AFs after the overexpression and knockdown of SIRT6, respectively. (G-H) Representative dihydroethidium staining images and relative fluorescence of rat AFs. (I-J) *In vitro* wound healing to determine cellular migration of AFs at 0 h and 24 h. (K) Representative immunofluorescence images of p62 (red) and LC3 (green) to examine autophagic flux of rat AFs. GAPDH was used as an endogenous control. n = 3–4 for each group except for B where n = 6. **, $P < 0.01$ compared with control group; ##, $P < 0.01$ compared with ATII + NC or ATII + rAAV-GFP group; $$, $P < 0.01$ compared with ATII + miR-122 inhibitor group. A.U., arbitrary units; R.E., relative expression; ATII, angiotensin II; AFs, adventitial fibroblasts; NC, negative control; SIRT6, sirtuin 6.

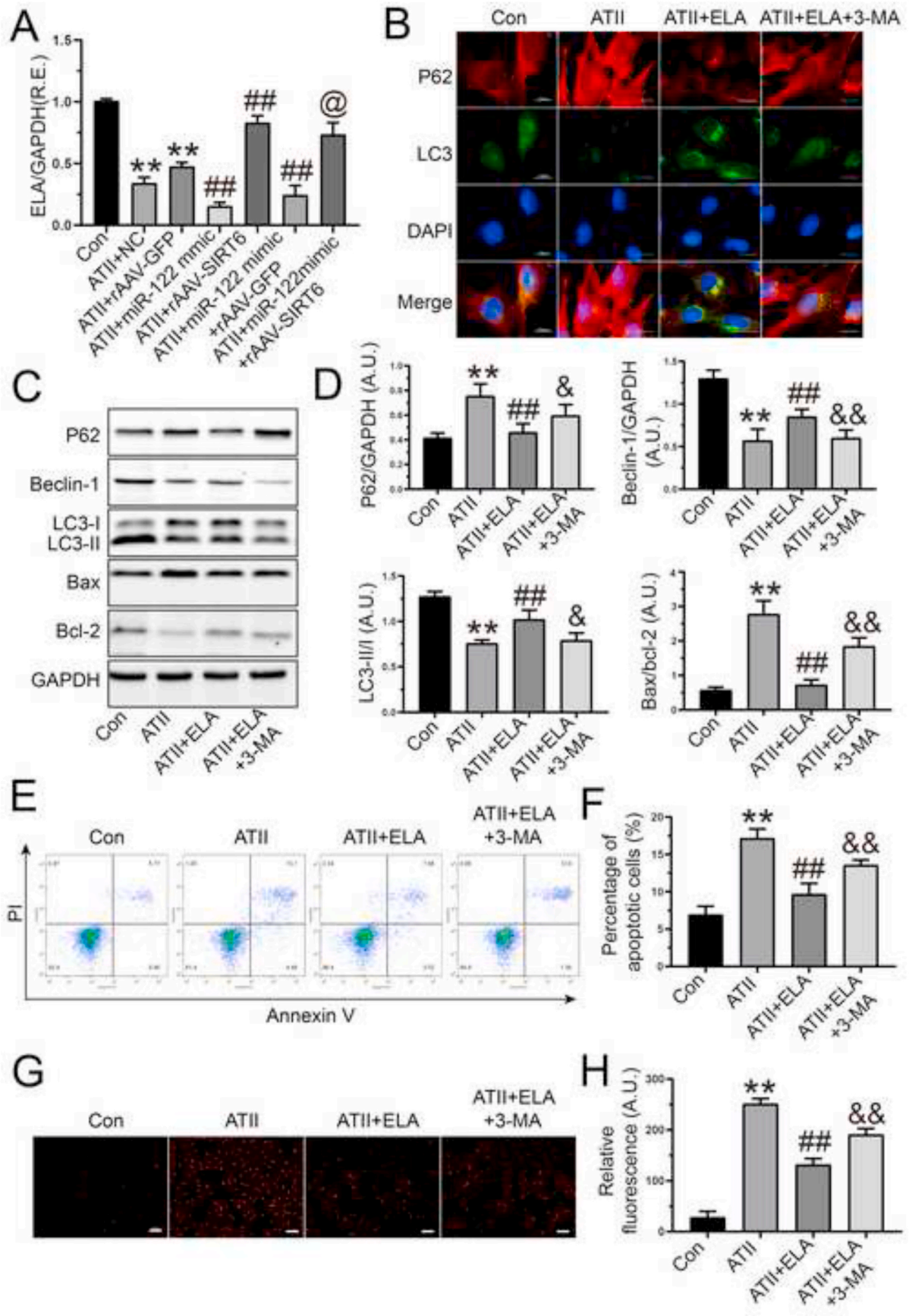

(caption on next page)

Fig. 5. ELA suppressed ATII-induced loss of autophagy and augmentation of apoptosis and oxidative stress in rat AFs. (A) The relative mRNA level of ELA was downregulated in rat AFs by miR-122-5p mimic but was upregulated with rAAV-SIRT6 treatment. (B) Representative immunofluorescence images of p62 (red) and LC3 (green) to examine autophagic flux of AFs. (C-D) Representative Western blots to determine the levels of p62, beclin-1, LC3, bax, and bcl-2 in rat AFs. GAPDH was used as an endogenous control. (E-F) Percentage of apoptotic cells with flow cytometry array. (G-H) Dihydroethidium staining to examine reactive oxygen species generation of AFs. n = 3–4 for each group except for A where n = 6. **, $P < 0.01$ compared with control group; ##, $P < 0.01$ compared with ATII or ATII + NC or ATII + rAAV-GFP group; &, $P < 0.05$, &&, $P < 0.01$ compared with ATII + ELA group; @, $p < 0.05$ compared with ATII + miR-122 mimic + rAAV-GFP group; A.U., arbitrary units; R.E., relative expression; ATII, angiotensin II; AFs, adventitial fibroblasts; 3-MA, 3-methyladenine; NC, negative control; ELA, elabela; SIRT6, sirtuin 6.

protein levels of SIRT6 in rat AFs, which were further reduced by miR-122-5p mimic (Fig. 4B and C) but was elevated by miR-122-5p inhibitor (Fig. 4B and D). Additionally, ATII-mediated loss of SIRT6 protein was rescued in rat AFs by SIRT6 overexpression (Fig. 4E) but was further reduced by SIRT6 siRNA (Fig. 4F). Moreover, both overexpression of SIRT6 and miR-122-5p inhibitor significantly prevented the ATII-induced promotion of oxidative stress (Fig. 4G and H), and cellular migration (Fig. 4I and J), and loss of autophagy (Fig. 4K) in rat AFs. Furthermore, the silencing of SIRT6 partially suppressed the protective roles of miR-122-5p inhibitor in the ATII-mediated the promotion of apoptosis (Fig. 3D and E), oxidative stress (Fig. 4G and H), cellular migration (Fig. 4I and J), and loss of autophagy (Fig. 4K) in rat AFs. Our data demonstrated that inhibition of miR-122-5p exerted the protective effects on ATII-mediated loss of autophagy and augmentation of oxidative stress and migration in rat AFs by targeting SIRT6 signaling.

3.5. Treatment with ELA suppressed ATII-mediated loss of autophagy and promotion of apoptosis and oxidative stress in rat AFs

We next investigated the regulatory roles of miR-122-5p and SIRT6 in ELA expression and interactions among miR-122-5p, SIRT6, and ELA in rat AFs. As expected, ATII-induced the downregulation of ELA expression was further reduced by miR-122-5p mimic but was elevated by SIRT6 overexpression (Fig. 5A). Intriguingly, treatment with rAAV-SIRT6 rescued miR-122-5p mimic-mediated the decline in the expression of ELA in rat AFs in response to ATII, suggesting that miR-122-5p negatively regulated ELA via the suppression of SIRT6 signaling (Fig. 5A). Then, we investigated the effects of ELA on ATII-mediated actions in rat AFs. Exogenous ELA stimulation inhibited ATII-mediated anti-autophagic action in rat AFs (Fig. 5B), which was accompanied by the upregulation of beclin-1 and LC3-II expression and the downregulation in the protein level of p62 (Fig. 5C and D). However, the pro-autophagic role of ELA in AFs was partially blocked by 3-methyladenine (Fig. 5B, C, and D). Moreover, treatment with ELA reduced bax/bcl-2 ratio (Fig. 5C and D) and prevented ATII-induced cellular apoptosis (Fig. 5E and F) and oxidative stress (Fig. 5G and H) in rat AFs, which were enhanced by 3-methyladenine. Thus, our data indicated the protective effects of ELA on ATII-mediated anti-autophagic, pro-apoptotic, and pro-oxidant actions in rat AFs, which may be regulated by the activation of miR-122-5p/SIRT6 signaling.

3.6. MiR-122-5p regulated apoptosis, oxidative stress, and autophagy in rat AFs via activating the SIRT6-ELA-ACE2 signaling

ACE2 serves as a negative regulator of the renin-angiotensin system (RAS) and a co-receptor for the severe acute respiratory syndrome coronavirus 2 (SARS-CoV-2) (Gheblawi et al., 2020; Patel et al., 2016; Sato et al., 2017; Zhong et al., 2010). In our previous study, we demonstrated a model of cross-talk between SIRT6 and ACE2 signaling in ATII-induced cardiovascular fibrosis and remodeling in hypertension (Zhang et al., 2017a). To investigate the inner link between miR-122-5p and the ELA-ACE2 signaling, ELA siRNA and ACE2 siRNA were transfected into rat AFs, respectively. The mRNA level of ELA (Fig. 6A) and the expression of ACE2 (Fig. 6B, C, and D) were significantly downregulated in AFs after the silencing of ELA and ACE2, respectively. Moreover, treatment with miR-122-5p inhibitor suppressed ATII-mediated promotion of cellular apoptosis (Fig. 6E and F), oxidant injury (Fig. 6G and H), and inflammatory response (Fig. 6I), and loss of autophagy (Fig. 6J) in rat AFs, which were partially reversed by co-transfection of ELA siRNA. Furthermore, stimulation with ATII induced a marked decrease in the protein level of ACE2 in rat AFs, which was elevated by the administration of ELA (Fig. 6K and L). Importantly, co-treatment with ACE2 siRNA inhibited ELA-mediated the upregulation in the expression of ACE2 (Fig. 6K and L) in rat AFs. Taken together, these data demonstrated that inhibition of miR-122-5p suppressed ATII-mediated pro-apoptotic, pro-oxidant, pro-inflammatory, and anti-autophagic effects in rat AFs by activating the SIRT6-ELA-ACE2 signaling (Fig. 7).

4. Discussion

In this study, we demonstrated for the first-time a cross-talk between miR-122-5p and the SIRT6-ELA-ACE2 signaling in controlling cellular apoptosis, migration, oxidative stress, and autophagy in rat AFs in response to ATII. The imbalance of apoptosis and autophagy and pathological hypertrophy of the blood vessel cells are the main causes of vascular remodeling of hypertension (Bersi et al., 2016; An et al., 2015; Intengan and Schiffrin, 2001). The adventitia cells play crucial roles in vascular remodeling, and excessive adventitial remodeling results in early aortic maladaptation in ATII-induced hypertension and TAC-induced vascular dysfunction (Bersi et al., 2016; Xu et al., 2016). The AFs, major cell components of adventitia, are considered to be sensors of vascular walls disruption and dysfunction and are early responders and activators of the blood vessel in response to injury or stress, which are linked with the activation of the RAS and the ELA/apelin-APJ axis (Yang et al., 2017; Xu et al., 2016; Sato et al., 2017). The mechanistic roles of ATII in vascular remodeling, including oxidative stress, apoptosis, and inflammation, have been increasingly appreciated (Heeneman et al., 2007; Bersi et al., 2016; Patel et al., 2016). Oxidative stress is involved in the apoptosis/autophagy imbalance and induces an inflammatory response of vascular cells (Huang et al., 2015). Autophagy sustains vascular health by reducing inflammation and apoptosis and by regulating vascular pathologies including arterial stiffness and hypertension (Huang and Klionsky, 2007; Shao et al., 2016). Increased autophagic activity enhances cell vitality and survival against pathophysiological stimuli in vascular cells. However, over-activation of autophagy in vascular cells has detrimental effects on cell survival and may lead to cellular death. Thus, autophagy mainly functions as a protective response by suppressing oxidative stress, apoptosis, and inflammation during vascular injury and disorders (Dalvi et al., 2016; Netea-Maier et al., 2016). The regulatory role of ATII in autophagy depends on different types of cells and diseases. Recently, ATII has been reported to suppress microtubule-associated protein 1 LC3-I-to-LC3-II conversion and decrease the number of autophagic vacuoles in skeletal muscular dystrophy, indicating that ATII reduces autophagic activity and prevents autophagosome formation (Silva et al., 2019). In this study, exposure to ATII induced a decline in autophagy and marked increases in apoptosis, oxidative stress, and inflammation in rat AFs, which were exacerbated by transfection of miR-122-5p mimic but were rescued with miR-122-5p inhibitor treatment. Moreover, 3-methyladenine, an autophagy inhibitor, was used to explore the relationship between autophagy and apoptosis. We demonstrated that in rat AFs stimulation with 3-methyladenine enhanced ATII-mediated cellular apoptosis along with increased bax/bcl-2 ratio, suggesting a

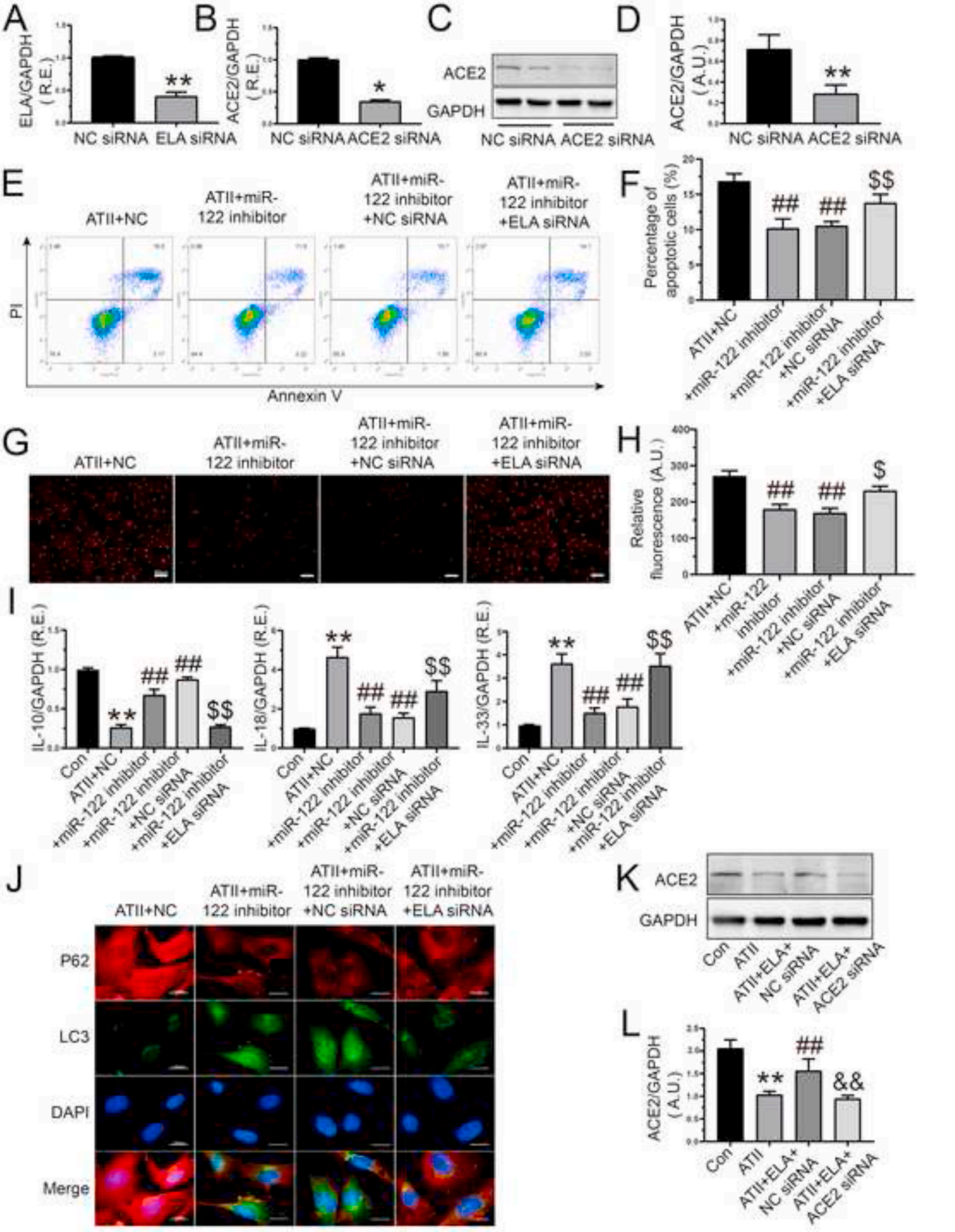

(caption on next page)

Fig. 6. Inhibition of miR-122-5p exerted the protective effects on ATII-mediated pro-apoptosis, pro-oxidant, pro-inflammation, and anti-autophagy via activating the ELA-ACE2 signaling in rat AFs. (A) The relative mRNA level of ELA was downregulated in AFs after the knockdown of ELA. (B-D) Decreased mRNA and protein levels of ACE2 were performed to ensure the effective transfection of ACE2 siRNA. (E-F) Percentage of apoptotic cells of AFs by flow cytometry analysis. (G-H) The production of oxidative stress in rat AFs by dihydroethidium staining. (I) Relative mRNA levels of IL-10, IL-18, and IL-33 in rat AFs. (J) Immunofluorescence images of p62 (red) and LC3 (green) to examine autophagic flux of rat AFs. (K-L) The expression of ACE2 in rat AFs in the absence and presence of ATII, ELA, and ACE2 siRNA, respectively. GAPDH was used as an endogenous control. n = 3–4 for each group except for I where n = 5–6. *, $P < 0.05$, **, $P < 0.01$ compared with control or NC siRNA group; ##, $P < 0.01$ compared with ATII or ATII + NC group; &&, $P < 0.01$ compared with ATII + ELA + NC siRNA group; $, $P < 0.05$, $$, $P < 0.01$ compared with ATII + miR-122 inhibitor + NC siRNA group. A.U., arbitrary units; R.E., relative expression; ATII, angiotensin II; AFs, adventitial fibroblasts; NC, negative control; ELA, elabela; ACE2, angiotensin-converting enzyme 2; IL-10, interleukin-10; IL-18, interleukin-18; IL-33, interleukin-33.

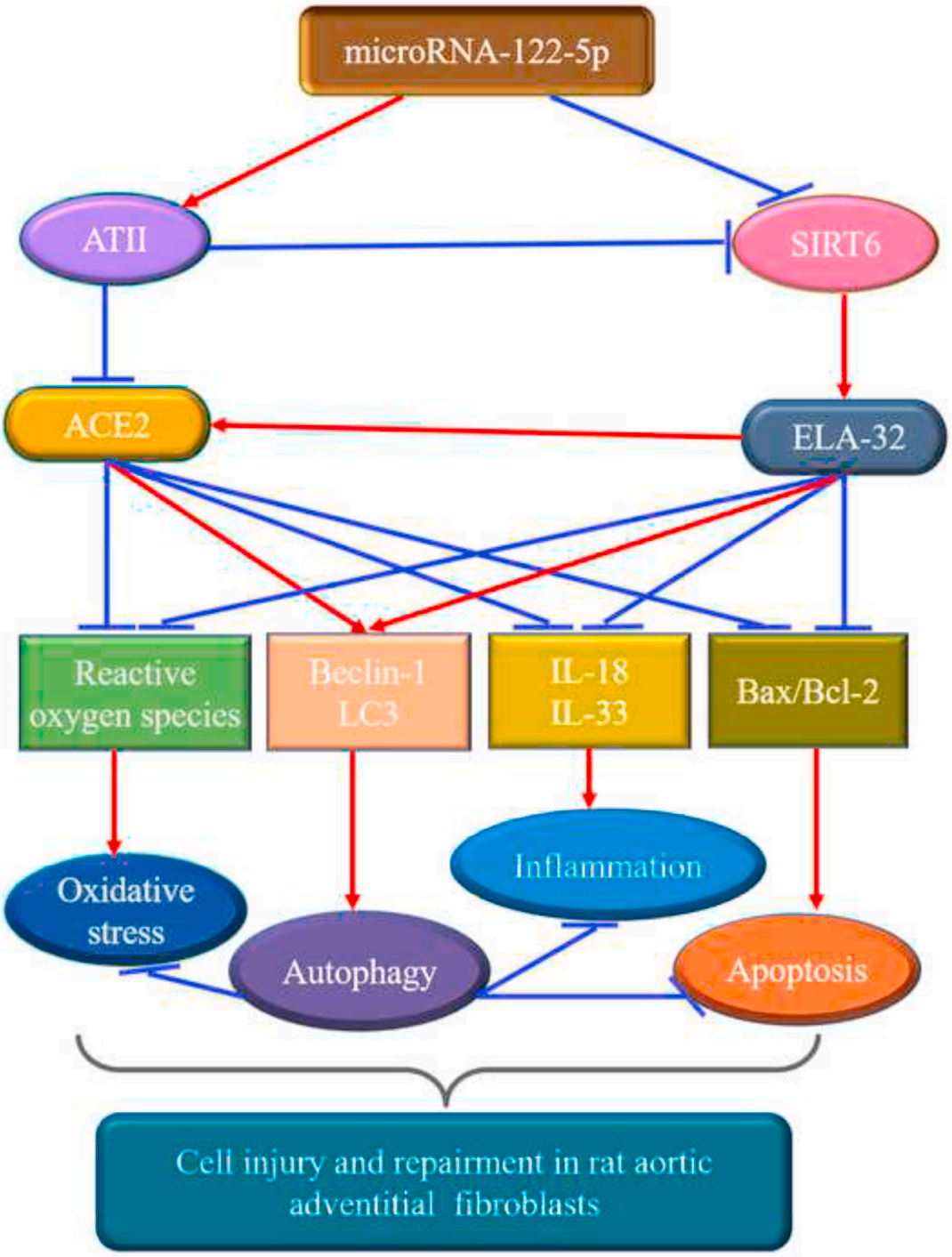

Fig. 7. Schematic overview of the crucial roles of miR-122-5p in rat aortic adventitial fibroblasts. MiR-122-5p serves as an important regulator of ATII-mediated loss of autophagy and promotion of apoptosis, oxidative stress, and inflammation in rat adventitial fibroblasts by modulating the SIRT6-Elabela-ACE2 signaling. ACE2, angiotensin-converting enzyme 2; ATII, angiotensin II; ELA, elabela; IL, interleukin; SIRT6, sirtuin 6.

negative correlation between autophagy and apoptosis.

Currently, the levels of miR-122 are significantly elevated in the hypertensive population and the aortic adventitia of hypertensive rats with vascular injury, indicating the adverse effect of miR-122 on aortic adventitial remodeling (Xu et al., 2016; Cengiz et al., 2015). Enhanced miR-122 contributes to endothelial dysfunction via promoting endothelial cell apoptosis by targeting X-linked inhibitor-of-apoptosis protein in ApoE$^{-/-}$ mice (Li et al., 2019). Importantly, miR-122 aggravates cell proliferation, apoptosis, and oxidative stress by PI3K/protein kinase B signaling in a rat model of renal ischemic-reperfusion injury and renal cells (Qu and Zhang, 2018; Fan et al., 2018). In our study, transfection of miR-122-5p mimic aggravated ATII-induced promotion of oxidative stress, cellular apoptosis and inflammation, and loss of autophagy in rat AFs. Conversely, the administration of miR-122-5p inhibitor ameliorated the ATII-mediated actions, suggesting that the inhibition of miR-122-5p was a protective factor in adventitial cell injury and dysfunction.

SIRT6 has emerged as a negative regulator of ATII-induced hypertension by preventing vascular inflammation, oxidant injury, and dysfunction (Zhang et al., 2017a; D'Onofrio et al., 2018; Lappas, 2012). Overexpression of SIRT6 promotes autophagic flux against atherosclerosis by reducing foam cell formation (He et al., 2017). In this study, we utilized two bioinformatics software to identify the binding sites between miR-122-5p and SIRT6 3′-UTR. To verify the bioinformatics-based prediction, we examined the SIRT6 expression in rat AFs after the transfection of miR-122-5p mimic and inhibitor. ATII-mediated loss of SIRT6 level was further reduced by miR-122-5p mimic but elevated by miR-122-5p inhibitor, indicating that SIRT6 was a direct target of miR-122-5p. Our data also demonstrated that SIRT6 inhibited ATII-induced augmentation of apoptosis, migration, oxidative stress, and loss of autophagic flux. Additionally, the overexpression of SIRT6 improved the mRNA level of ELA in rat AFs in response to ATII. Importantly, the pro-autophagic, anti-apoptotic, anti-oxidant, and anti-inflammatory roles of miR-122-5p inhibitor were suppressed by SIRT6 and ELA knockdown, supporting that the beneficial effects of miR-122-5p inhibition on ATII-induced actions in rat AFs were mediated via the activation of SIRT6-ELA signaling.

Apelinergic system, including APJ and its two classes of endogenous ligands, named ELA and apelin, has received increasing attention for its potential therapeutic target in cardiovascular disorders (Yang et al., 2017; Zhang et al., 2017a; Xu et al., 2016). ELA exerts cardiovascular protective effects in APJ-dependent manner. The ELA/apelin-APJ system has been shown to relax aortic blood vessels and reduce systolic blood pressure by enhancing the expression of ACE2 (Sato et al., 2017). ACE2, an endogenous RAS blocker by its actions on the Mas receptor, is a key target for apelinergic system to oppose the molecular and cellular actions of ATII and exert cardiovascular protective effects (Gheblawi et al., 2020; Patel et al., 2016; Zhong et al., 2010; Ma et al., 2020; Song et al., 2020). The reduced level of ACE2 has been found in patients with the novel coronavirus disease 2019 (COVID-19) after entry of SARS-CoV-2 into cells and in worsened pathological vascular remodeling and dysfunction during hypertension (Gheblawi et al., 2020; Patel et al., 2016). Our previous work and other studies have reported that the exogenous replenishment of apelin or SIRT6 upregulates the expression of ACE2 and disrupts the balance between ACE and ACE2 during hypertension and heart failure (Zhang et al., 2017a; Patel et al., 2016). However, ELA reduces the ratio of ACE/ACE2 differently from apelin to affect the RAS activation (Sato et al., 2017; Ma et al., 2020), indicating that the ELA-APJ-ACE2 axis represents a protective pathway in cardiovascular homeostasis. In this work, the expression of ELA was significantly downregulated in rat AFs after stimulation with ATII. Moreover, administration of ELA promoted autophagic flux and inhibited cellular oxidative stress and apoptosis in rat AFs in response to ATII. Additionally, the pro-autophagic, anti-oxidant, and anti-apoptotic effects of ELA in rat AFs were partially prevented by 3-methyladenine. Since SIRT6 is a direct target for miR-122-5p regulation, we investigated the interactions between miR-122-5p and the SIRT6-ELA-ACE2 signaling. Notably, treatment with miR-122-5p mimic accelerated ATII-induced decline in the level of ELA in rat AFs, which was elevated by SIRT6 overexpression, indicating that miR-122-5p negatively regulated ELA via the modulation of SIRT6 signaling. Furthermore, we determined the direct effects of miR-122-5p on ELA by co-transfecting ELA siRNA into rat AFs. The beneficial effects of miR-122-5p inhibition on controlling autophagy, apoptosis, and oxidative stress in rat AFs were suppressed by ELA siRNA. Finally, the protein level of ACE2 was reduced in rat vascular AFs after treatment with ATII, which was remarkably enhanced by exogenous replenishment of ELA. However, the knockdown of ACE2 with siRNA inhibited ELA-mediated increase in the expression of ACE2 in rat AFs. To our knowledge, this is the first report to describe the cross-talk among miR-122-5p, RAS, apelinergic system, and SIRT6 signaling in the modulation of apoptosis, oxidative stress, and autophagy in the cardiovascular system.

In summary, our findings demonstrated that miR-122-5p inhibition exerts beneficial effects by potentiating autophagy and blocking apoptosis, oxidative stress, and inflammation in rat aortic AFs via the activation of SIRT6-ELA-ACE2 signaling. Therefore, our study provides definite evidence that miR-122-5p may be a novel predictive biomarker of adventitial injury and vascular remodeling and that targeting the SIRT6-ELA-ACE2 signaling has potential therapeutic importance for controlling vascular remodeling and dysfunction. Further studies are still required to precisely clarify the exact regulatory mechanisms of the cross-talk between miR-122-5p and the SIRT6-ELA-ACE2 signaling pathway in adventitial injury and related vascular disorders.

Data availability statement

The datasets generated and analyzed in the current study are available from the corresponding author upon reasonable request.

CRediT authorship contribution statement

Juan-Juan Song: Conceptualization, Methodology, Software, Data curation, Formal analysis, Investigation, Writing - original draft, Visualization, Writing - review & editing. **Mei Yang:** Formal analysis, Data curation, Investigation, Methodology, Software, Writing - original draft. **Ying Liu:** Formal analysis, Data curation, Writing - original draft. **Jia-Wei Song:** Formal analysis, Data curation, Writing - original draft. **Juan Wang:** Visualization, Investigation. **Hong-Jie Chi:** Visualization, Investigation. **Xiao-Yan Liu:** Visualization, Investigation. **Kun Zuo:** Supervision, Software, Validation. **Xin-Chun Yang:** Supervision, Software, Validation. **Jiu-Chang Zhong:** Conceptualization, Project administration, Funding acquisition, Supervision, Resources, Data curation, Writing - original draft, Writing - review & editing.

Declaration of competing interest

All the authors declare that they have no conflict of interest.

Acknowledgments

This study was supported by the General Program and the National Major Research Plan Training Program of the National Natural Science Foundation of China (No. 81770253; 91849111; 81370362; 81900382; 91339108; 81670214) and the Talent Project of Beijing Chaoyang Hospital Affiliated to Capital Medical University in China (No. 20180118).

Appendix A. Supplementary data

Supplementary data to this article can be found online at https://doi.org/10.1016/j.ejphar.2020.173374.

References

An, S.J., Liu, P., et al., 2015. Characterization and functions of vascular adventitial fibroblast subpopulations. Cell. Physiol. Biochem. 35 (3), 1137–1150. https://doi.org/10.1159/000373939.

Bersi, M.R., Bellini, C., et al., 2016. Excessive adventitial remodeling leads to early aortic maladaptation in angiotensin-induced hypertension. Hypertension 67 (5), 890–896. https://doi.org/10.1161/HYPERTENSIONAHA.115.06262.

Cengiz, M., Karatas, O.F., et al., 2015. Differential expression of hypertension- associated microRNAs in the plasma of patients with white coat hypertension. Medicine (Baltim.) 94 (13), e693. https://doi.org/10.1097/MD.0000000000000693.

Dalvi, P., Sharma, H., et al., 2016. Enhanced autophagy in pulmonary endothelial cells on exposure to HIV-Tat and morphine: role in HIV-related pulmonary arterial hypertension. Autophagy 12 (12), 2420–2438. https://doi.org/10.1080/15548627.2016.1238551.

De Rosa, S., Indolfi, C., 2015. Circulating microRNAs as biomarkers in cardiovascular diseases. Experientia Suppl. 106, 139–149. https://doi.org/10.1007/978-3-0348-0955-9_6.

D'Onofrio, N., Servillo, L., et al., 2018. SIRT1 and SIRT6 signaling pathways in cardiovascular disease protection. Antioxidants Redox Signal. 28 (8), 711–732. https://doi.org/10.1089/ars.2017.7178.

Elhanati, S., Ben-Hamo, R., et al., 2016. Reciprocal regulation between SIRT6 and mir-122 controls liver metabolism and predicts hepatocarcinoma prognosis. Cell Rep. 14 (2), 234–242. https://doi.org/10.1016/j.celrep.2015.12.023.

Fan, Y., Ma, X., et al., 2018. miR-122 promotes metastasis of clear-cell renal cell carcinoma by downregulating Dicer. Int. J. Canc. 142 (3), 547–560. https://doi.org/10.1002/ijc.31050.

Gheblawi, M., Wang, K., et al., 2020. Angiotensin converting enzyme 2: SARS-CoV- 2 receptor and regulator of the renin-angiotensin system-Celebrating the 20th anniversary of the discovery of ACE2. Circ. Res. 126 (10), 1457–1475. https://doi.org/10.1161/CIRCRESAHA.120.317015.

He, J., Zhang, G., et al., 2017. SIRT6 reduces macrophage foam cell formation by inducing autophagy and cholesterol efflux under ox-LDL condition. FEBS J. 284 (9), 1324–1337. https://doi.org/10.1111/febs.14055.

Heeneman, S., Sluimer, J.C., et al., 2007. Angiotensin-converting enzyme and vascular remodeling. Circ. Res. 101 (5), 441–454. https://doi.org/10.1161/CIRCRESAHA.107.148338.

Huang, J., Klionsky, D.J., 2007. Autophagy and human disease. Cell Cycle 6 (15), 1837–1849. https://doi.org/10.4161/cc.6.15.4511.

Huang, S., Lu, W., et al., 2015. A new microRNA signal pathway regulated by long noncoding RNA TGFB2-OT1 in autophagy and inflammation of vascular endothelial cells. Autophagy 11 (12), 2172–2183. https://doi.org/10.1080/15548627.2015.1106663.

Hynes, C.J., Clancy, J.L., et al., 2012. miRNAs in cardiac disease: sitting duck or moving target? IUBMB Life 64 (11), 872–878. https://doi.org/10.1002/iub.1082.

Intengan, H.D., Schiffrin, E.L., 2001. Vascular remodeling in hypertension: roles of apoptosis, inflammation. and fibrosis. Hypertension 38 (3), 581–587. https://doi.org/10.1161/hy09t1.096249.

Kataoka, M., Wang, D.Z., 2014. Non-coding RNAs including miRNAs and LncRNAs in cardiovascular biology and disease. Cells 3 (3), 883–898. https://doi.org/10.3390/cells3030883.

Lappas, M., 2012. Anti-inflammatory properties of sirtuin 6 in human umbilical vein endothelial cells. Mediat. Inflamm. 2012, 597514. https://doi.org/10.1155/2012/597514.

Li, Y., Yang, N., et al., 2019. MicroRNA-122 promotes endothelial cell apoptosis by targeting XIAP: therapeutic implication for atherosclerosis. Life Sci. 232, 116590. https://doi.org/10.1016/j.lfs.2019.116590.

Ma, Z., Song, J.J., et al., 2020. The Elabela-APJ axis: a promising therapeutic for heart failure. Heart Fail. Rev. 26, 1–10. https://doi.org/10.1007/s10741-020-09957-5.

Netea-Maier, R.T., Plantinga, T.S., et al., 2016. Modulation of inflammation by autophagy: consequences for human disease. Autophagy 12 (2), 245–260. https://doi.org/10.1080/15548627.2015.1071759.

Patel, V.B., Zhong, J.C., et al., 2016. Role of the ACE2/angiotensin 1-7 Axis of the renin-angiotensin system in heart failure. Circ. Res. 118 (8), 1313–1326. https://doi.org/10.1161/CIRCRESAHA.116.307708.

Qu, X.H., Zhang, K., 2018. MiR-122 regulates cell apoptosis and ROS by targeting DJ-1 in renal ischemic reperfusion injury rat models. Eur. Rev. Med. Pharmacol. Sci. 22 (24), 8830–8838. https://doi.org/10.26355/eurrev_201812_16651.

Ridker, P.M., Hennekens, C.H., et al., 2000. C-reactive protein and other markers of inflammation in the prediction of cardiovascular disease in women. N. Engl. J. Med. 342 (12), 836–843. https://doi.org/10.1056/NEJM200003233421202.

Sato, T., Sato, C., et al., 2017. ELABELA-APJ axis protects from pressure overload heart failure and angiotensin II-induced cardiac damage. Cardiovasc. Res. 113 (7), 760–769. https://doi.org/10.1093/cvr/cvx061.

Shao, B.Z., Han, B.Z., et al., 2016. The roles of macrophage autophagy in atherosclerosis. Acta Pharmacol. Sin. 37 (2), 150–156. https://doi.org/10.1038/aps.2015.87.

Silva, K.A.S., Ghiarone, T., et al., 2019. Angiotensin II suppresses autophagy and disrupts ultrastructural morphology and function of mitochondria in mouse skeletal muscle. J. Appl. Physiol. 126 (6), 1550–1562. https://doi.org/10.1152/japplphysiol.00898.2018.

Song, J.J., Ma, Z., et al., 2020. Gender differences in hypertension. J. Cardiovasc. Transl. Res. 13 (1), 47–54. https://doi.org/10.1007/s12265-019-09888-z.

Xu, R., Zhang, Z.Z., et al., 2016. Ascending aortic adventitial remodeling and fibrosis are ameliorated with Apelin-13 in rats after TAC via suppression of the miRNA-122 and LGR4-β-catenin signaling. Peptides 86, 85–94. https://doi.org/10.1016/j.peptides.2016.10.005.

Yang, P., Read, C., et al., 2017. Elabela/Toddler Is an endogenous agonist of the apelin/APJ receptor in the adult cardiovascular system, and exogenous administration of the peptide compensates for the downregulation of its expression in pulmonary arterial hypertension. Circulation 135 (12), 1160–1173. https://doi.org/10.1161/CIRCULATIONAHA.116.023218.

Yang, Y., Tian, T., et al., 2019. SIRT6 protects vascular endothelial cells from angiotensin II-induced apoptosis and oxidative stress by promoting the activation of Nrf2/ARE signaling. Eur. J. Pharmacol. 859, 172516. https://doi.org/10.1016/j.ejphar.2019.172516.

Zhang, Z.Z., Cheng, Y.W., et al., 2017a. The sirtuin 6 prevents angiotensin II-mediated myocardial fibrosis and injury by targeting AMPK-ACE2 signaling. Oncotarget 42 (8), 72302–72314. https://doi.org/10.18632/oncotarget.20305.

Zhang, Z.Z., Wang, W., et al., 2017b. Apelin is a negative regulator of angiotensin II-mediated adverse myocardial remodeling and dysfunction. Hypertension 70 (6), 1165–1175. https://doi.org/10.1161/HYPERTENSIONAHA.117.10156.

Zhong, J., Basu, R., et al., 2010. Angiotensin-converting enzyme 2 suppresses pathological hypertrophy, myocardial fibrosis, and cardiac dysfunction. Circulation 122 (7), 717–728. https://doi.org/10.1161/CIRCULATIONAHA.110.955369.